MOLECULAR AND CELLULAR BIOLOGY, July 1995, p. 3796–3804 Vol. 15, No. 7
0270-7306/95/$04.00+0

Rapid mRNA Degradation Mediated by the c-*fos* 3′ AU-Rich Element and That Mediated by the Granulocyte-Macrophage Colony-Stimulating Factor 3′ AU-Rich Element Occur through Similar Polysome-Associated Mechanisms

ERIC WINSTALL, MARIE GAMACHE,† AND VINCENT RAYMOND*

Laboratoire d'Endocrinologie Moléculaire, Centre de Recherche du Centre Hospitalier de l'Université Laval, Québec, Québec G1V 4G2, Canada

Received 7 February 1995/Returned for modification 10 April 1995/Accepted 26 April 1995

The different 3′ noncoding AU-rich elements (ARE) that mediate the degradation of many short-lived mRNAs may function through distinct decay pathways; translation-dependent and -independent mechanisms have been proposed. To investigate the cotranslational model, we designed an expression system that exploits the properties of the ferritin iron-responsive element to shuttle chimeric mRNAs from ribonucleoproteins to polyribosomes. The iron-responsive element was introduced in the 5′ untranslated regions of α-globin mRNAs that harbored in their 3′ untranslated regions either the c-*fos* ARE or the granulocyte-macrophage colony-stimulating factor ARE as prototypes of the different ARE subsets. The cytoplasmic location of the transcripts was controlled by intracellular iron availability and monitored by polysomal profile analysis. We report that these two mRNA subsets behaved identically in this system. Iron deprivation by desferrioxamine treatment stabilized both transcripts by sequestering them away from polyribosomes. Sequential treatments with desferrioxamine, followed by hemin to concentrate the mRNAs in the ribonucleoprotein pool prior to translation, showed that rapid degradation occurred only upon redistribution of the transcripts to polyribosomes. Deletion of a critical cytosine in the iron-responsive element abolished targeted sequestration and restored high-level constitutive mRNA instability. These observations demonstrate that the c-*fos* and granulocyte-macrophage colony-stimulating factor ARE subsets mediate selective mRNA degradation through similar polysome-associated mechanisms coupled with ongoing translation.

Among the specific posttranscriptional mechanisms that have evolved to regulate the pattern of gene expression in higher eukaryotes, control of mRNA stability plays a predominant role. For instance, the high-level lability of an mRNA allows rapid downregulation of protein synthesis after arrest of transcription and thus provides an efficient mechanism for transient expression. This mode of regulation is a key feature of many early-response genes involved in developmental processes (3, 21, 22, 52), and deregulation of this control mechanism sometimes leads to neoplastic transformation (33, 47).

Several types of eukaryotic mRNA instability determinants in the coding regions and 3′ untranslated regions (UTR) of many transiently expressed mRNAs have been identified (3, 21). One of these determinants is a 50- to 100-nucleotide (nt) sequence composed mainly of adenylate and uridylate residues. This element, named the AU-rich element (ARE), is usually found in the 3′ UTR of many short-lived transcripts encoding the lymphokines, several proto-oncogenes, and some transcriptional factors (14, 21, 58). Shaw and Kamen were the first to show that the 51-nt ARE located in the 3′ UTR of the human granulocyte-macrophage colony-stimulating factor (GM-CSF) mRNA functions as a *cis*-acting destabilizing sequence (58). Insertion of the GM-CSF ARE into the 3′ UTR of β-globin mRNA dramatically reduced the half-life of the otherwise stable β-globin messenger from 17 h to less than 30 min (58). More recent experiments established that the different AREs located in the c-*fos*, c-*myc*, beta interferon, cyclic AMP-responsive element modulator, and urokinase-type plasminogen activator messengers also function as mRNA-destabilizing elements (2, 17, 27, 46, 59). Following the description of the presence of various copies of the AUUUA pentamer repeated several times within an AU-rich region (reviewed in references 21 and 52), extensive mutational analysis revealed that two interdependent domains lie within the c-*fos* 70-nt ARE (59) and that the nonamer UUAUUUAUU (69) and its highly homologous motif UUAUUUA(U/A)(U/A) (32) are the key AREs mediating rapid mRNA decay. Regions surrounding the AREs also contribute to their efficiency. For instance, linker substitution mutagenesis showed that a region located 160 nt upstream of the 5′ end of a GM-CSF AU-rich sequence hinders the efficiency of the ARE following changes in cellular metabolism (25).

These findings, combined with the observation that the turnover of c-*fos* and GM-CSF mRNAs could be differentially regulated in the same cell line (57), suggested that the different AREs could be divided into two functionally distinct subtypes. The first ARE subset was identified in messengers in which turnover rates are altered following changes of hormonal status, cell growth conditions, or second-messenger induction. This subset includes ARE-containing mRNAs like the cytokine, interferon, and urokinase-type plasminogen activator messengers that are stabilized by cell-signaling pathways (35, 44, 45, 58) and the interleukin 3 mRNA that is destabilized when cyclosporin A is added to tumor cell lines (43). The

* Corresponding author. Mailing address: Laboratory of Molecular Endocrinology, CHUL Research Center, 2705 Laurier Blvd., Québec, Québec G1V 4G2, Canada. Phone: (418) 654-2296. Fax: (418) 654-2761. Electronic mail address: raymond@adn.chul.uquebec.ca.

† Present address: Unité de Médecine Génétique et Moléculaire, Centre de Recherche du Centre Hospitalier de l'Université Laval, Québec, Québec G1V 4G2, Canada.

second subset of ARE-containing mRNAs is depicted by the c-*fos*, c-*myc*, and cyclic AMP-responsive element modulator mRNAs, which do not respond to such signals (57, 61). The search for the *trans*-acting factors that participate in the destabilization of their target transcripts or, conversely, prevent their degradation has led to the identification of more than eight ARE-binding complexes (reviewed in reference 21). Some of these protein factors show constitutive binding properties, whereas others are inducible and bind to more specific regions of the AREs contained in the lymphokines, c-*fos*, or c-*myc* mRNAs.

Although much knowledge has been gained about the *cis*- and *trans*-acting elements involved in rapid mRNA destabilization, the molecular interactions between these elements and the cellular compartments where these interacting events occur are still poorly defined. A potential link between ARE-mediated mRNA degradation and translation first emerged from in vitro studies showing that protein synthesis inhibitors, like cycloheximide and puromycin, superinduced the accumulation of c-*fos*, c-*myc*, and GM-CSF transcripts (36, 40, 58). These early observations suggested either the participation of a labile *trans*-acting protein in rapid mRNA degradation or the requirement of translation for destabilization. Short time course in vitro experiments with cycloheximide subsequently supported the suggestion that c-*fos* mRNA degradation requires ongoing translation (65), whereas cell-free systems constituted of postribosomal supernatant extracts implied that labile cytosolic factors are part of the decay mRNA machinery (10, 12).

To distinguish between translation coupling and the presence of a labile nuclease(s), novel approaches have been designed to alleviate the need for adding protein synthesis inhibitors to in vitro systems. Using chimeric mRNAs containing a GM-CSF ARE cloned downstream of the hepatitis B virus S-antigen coding region, Aharon and Schneider recently demonstrated that poorly translated messengers, by virtue of the introduction of a stable secondary structure in their 5′ UTR, were not effectively targeted for selective destabilization. Insertion of a poliovirus internal ribosome entry site between the 5′ secondary structure and the initiation codon restored rapid mRNA turnover, suggesting that degradation was coupled to either ribosome binding or ongoing translation (1). On the other hand, Koeller et al., using the ferritin iron-responsive element (IRE) to regulate the translation of an mRNA encoding the transferrin receptor coding region attached to the c-*fos* ARE, found no stabilization of these labile transcripts upon arrest of translation (30). Their results support a model in which transactive labile proteins may be responsible for rapid mRNA turnover. The presence of two distinct degradative pathways, each specific for a particular ARE subset, might explain these divergent observations. Alternatively, the different systems used in these two sets of experiments may express particular stability and/or instability determinants.

To investigate the specificity of the pathways involved in ARE-mediated mRNA degradation, we designed a transient expression system in which the human ferritin IRE was introduced at an optimal position to efficiently control the translation of well-characterized α-globin constructs containing either a c-*fos* or a GM-CSF ARE. Experiments involving thorough manipulation of intracellular iron availability were combined with polysomal profile analysis to closely monitor the translocation of these chimeric mRNAs from ribonucleoprotein (RNP) pools to translationally active polyribosomes. Herein, we report that iron deprivation stabilized both sets of chimeric mRNAs by sequestering them in the RNP pool, whereas redistribution of these mRNAs to polyribosomes fully restored the destabilizing activity of the AREs. These observations provide the first direct evidence that these two distinct ARE subsets mediate selective mRNA degradation through similar polysome-associated mechanisms.

MATERIALS AND METHODS

Plasmid constructions. All plasmid DNA manipulations were performed according to standard protocols (55). The parental plasmids pαG, pαG-*fos*, and pαG-58+, which were used for subsequent subcloning of the IRE, have been described previously (47). Briefly, the α-globin–*fos* (pαG-*fos*) plasmid resulted from insertion of a 201-bp *Nsi*I-to-*Tth*111I fragment (position 3289 to 3489 [62]) obtained from the mouse c-*fos* gene and introduced into the unique *Bal*I site of the human α-globin expression plasmid pαG (an α-globin *Pst*I-to-*Pst*I [914-bp] fragment cloned into the *Pst*I site of pUC19). Plasmid pαG-58+ was constructed by blunt-end ligation of the synthesized, annealed, complementary 58-mer AT-rich oligonucleotide, as previously described (58), into the *Bal*I site of pαG.

Plasmids pIRE-αG-*fos* and pIRE-αG-58+ result from the insertion in pαG-*fos* and pαG-58+, respectively, of a 56-bp synthetic double-stranded oligonucleotide (shown in Fig. 1) containing the 44-bp human ferritin IRE and 12 adjacent residues, at the *Nco*I site 6 bp upstream of the initiation codon of α-globin. pIREM-αG-*fos* and pIREM-αG-58+ were constructed in an identical fashion, except that a point deletion was introduced during oligonucleotide synthesis in the IRE sequence, leaving a mutant form of IRE in which the conserved 5′ cytosine of the loop is absent (see Fig. 1). This kind of mutation prevents efficient binding of the IRE-binding protein (IRE-BP) to the IRE (49). DNA sequencing analysis revealed that the site necessary for efficient initiation of translation was retained, the original initiation codon was conserved, and no artifactual AUG codon was generated.

The plasmid pSIRE used for synthesis of RNA probes was constructed by ligation of a 296-nt *Sma*I-to-*Sma*I fragment obtained from pIRE-αG-*fos* into the *Sma*I site of pGEM-3. This insertion contains the first exonic sequences of the α-globin gene and the IRE. A description of the pSP62PLIHβ350 construct used for synthesis of the β-globin riboprobe has been published elsewhere (39).

Cells and transient DNA transfections. Mouse NIH 3T3 TK$^-$ cells were grown in Dulbecco modified Eagle's medium (DMEM) supplemented with 10% fetal calf serum. Cells at 50% confluence in a 10-cm-diameter culture dish were transfected by the calcium phosphate coprecipitation method (9, 20) and exposed to the precipitate for 16 h. Transfection samples contained 12.5 μg of test plasmid DNA and 1.5 μg of pHβ1, which served as a transfection control for subsequent mRNA quantitation. After the precipitate was washed, the cells were incubated for a further 24-h period in DMEM containing 10% fetal calf serum. Where indicated, desferrioxamine (Desferal; CIBA) was added directly to the cellular milieu to reach a final concentration of 100 μM. The cells were incubated in the presence of the iron chelator for 18 h. Actinomycin D (actinomycin C1; Boehringer) was then added to the cultures to achieve a final concentration of 10 μg/ml, and incubation was continued for various times ranging from 15 to 120 min. Where mentioned, desferrioxamine-treated cells were washed and incubated with DMEM supplemented with 10% fetal calf serum, 10 μg of actinomycin D per ml, and 100 μM hemin (Sigma) for periods varying from 15 to 120 min before RNA harvesting.

RNA decay analysis. Total cytoplasmic RNA was prepared by lysis of cells in Nonidet P-40 as described by Favaloro et al. (16). The pSIRE and pSP62PLIHβ350 plasmids were linearized with *Hin*dIII and *Eco*RI, respectively, and the resulting fragments were purified from a 1% agarose gel (Gene Clean, Bio 101). Uniformly ^{32}P-labeled probes were then synthesized, using T7 (pSIRE) or SP6 (pSP62PLIHβ350) RNA polymerase according to established protocols (4). Samples of cytoplasmic RNA (10 μg) and yeast tRNA (40 μg) were mixed with probes (100 μCi/μg), denatured at 85°C for 7 min, and hybridized at 50°C for at least 15 h. RNase treatment was then performed with 40 μg of RNase A (Boehringer) per ml and 700 U of RNase T_1 (Bethesda Research Laboratories) per ml for 45 min at 30°C. These RNase conditions precluded any intramolecular reannealing of the IRE stem-loop structure (see, for example, Fig. 2A). Nuclease-resistant fragments were fractionated on urea–6% polyacrylamide sequencing gels. As approximate DNA size markers, ^{32}P-labeled *Msp*I-digested DNA fragments of pBR322 were run on all analytical gels. The sizes of the protected fragments are presented in Results. In all experiments, the intensities of the protected fragments were measured by densitometric scanning, standardized by using the β-globin signal, and plotted.

Analysis of polysomal distributions. Duplicate dishes (diameter, 10 cm) of 50 to 60% confluent NIH 3T3 cells were transiently transfected with appropriate plasmids as described in Results. Cells were lysed by the addition of 400 μl of polysome lysis buffer (10 mM Tris-HCl [pH 8.4], 10 mM NaCl, 1.5 mM $MgCl_2$, 0.5% [vol/vol] Nonidet P-40). Nuclei were pelleted at 2,000 × *g*, and the resulting supernatants were layered on a 15 to 40% (wt/vol) linear sucrose gradient in polysome gradient buffer (10 mM Tris-HCl [pH 8.4], 10 mM NaCl, 1.5 mM $MgCl_2$). Gradients were centrifuged at 32,500 rpm for 2.5 h at 5°C in a Sorvall TH 641 rotor, and 400-μl fractions were collected with an Isco model 185 density-gradient fractionator connected to an Isco type 6 optical unit and a UA5 absorbance monitor. Protein content was monitored at 254 nm. To measure RNA, all fractions were treated with proteinase K (200 μg/ml), phenol extracted,

and ethanol precipitated (16). RNA was pelleted by centrifugation, resuspended in RNA hybridization buffer {80% [vol/vol] formamide, 40 mM PIPES [piperazine-*N*,*N*′-bis(2-ethanesulfonic acid)] [pH 6.7], 400 mM NaCl, 1 mM EDTA}, and hybridized with the appropriate riboprobes. RNase protection assays were performed as described above.

RESULTS

Design of an in vitro system to assess coupling of mRNA degradation with translation. Key experiments have led to the characterization of multiple IREs present in the mRNAs encoding several genes essential for iron homeostasis (for a review, see reference 15). Depending on their location in these messengers, IREs are capable of mediating two distinct post-transcriptional regulatory events. The IREs in the 3′ UTR of the mRNA encoding the human transferrin receptor participate in blocking messenger degradation (41), whereas those in the 5′ UTR of the mRNA encoding the iron storage protein ferritin or the heme biosynthesis enzyme erythroid 5-aminolevulinic-acid synthethase regulate mRNA translation (23, 24). More specifically, inhibition of translation occurs when iron concentrations are reduced. Ferritin mRNA is then sequestered in the cytoplasm through the interaction of IRE with IRE-BP, a translational repressor that interferes with an early, cap-dependent step prior to binding of the 43S preinitiation complex to the mRNA (for a review, see reference 29). When iron is added to the extracellular milieu, IRE-BP loses its affinity for IRE, and ferritin mRNA shifts from the RNP pool to active polysomes (15, 23, 24).

To investigate the existence of potentially distinct ARE-mediated decay pathways, we exploited the properties of the human ferritin IRE to control the translation of chimeric mRNAs containing two prototypes of the different ARE subsets. As shown in Fig. 1, the human ferritin H chain IRE was subcloned into the 5′ UTR of the α-globin recombinants, pαG-*fos* and pαG-58+, harboring AT-rich sequences obtained, respectively, from the human c-*fos* and GM-CSF genes. These two parental constructs have been studied extensively, and both displayed half-lives of less than 25 min in exponentially growing cells. Such short half-lives are conferred exclusively by insertion of the AREs in their 3′ UTR (47, 50). Because efficient inhibition of translation by an IRE requires its presence within 50 to 60 nt of the 5′ cap site (19), a convenient *Nco*I site, 35 nt downstream of the 5′ end of the message and 6 nt upstream of the α-globin initiation codon, was selected to introduce into the parental recombinants a 56-nt synthetic oligonucleotide. The oligomer encompassed a 44-nt ferritin IRE structure at its 5′ end (49), followed by 12 residues chosen to retain the sequences necessary for efficient initiation of translation (31). In this process, no artifactual AUG codons were generated. The new constructs were named pIRE-αG-*fos* and pIRE-αG-58+. To measure the levels of the various transcripts simultaneously, we also designed a 5′ riboprobe by subcloning the first exon of pIRE-αG-*fos* into a T7 expression vector (Fig. 1). This probe was named pSIRE.

Messenger sequestration prevents rapid mRNA degradation mediated by 3′ AREs. Using the IRE shuttling system, we first investigated the presence of short-lived soluble nucleases that would be recognized by detection of the rapid turnover of the chimeric mRNAs under conditions of low intracellular iron availability.

Plasmids pIRE-αG-*fos* and pIRE-αG-58+ were transfected independently into NIH 3T3 cells along with a β-globin construct (plasmid pHβI) as the control for monitoring transfection efficiency and mRNA recovery; pHβI did not harbor any shuttling or instability determinant. To induce messenger sequestration, we used the drug desferrioxamine, which, unlike

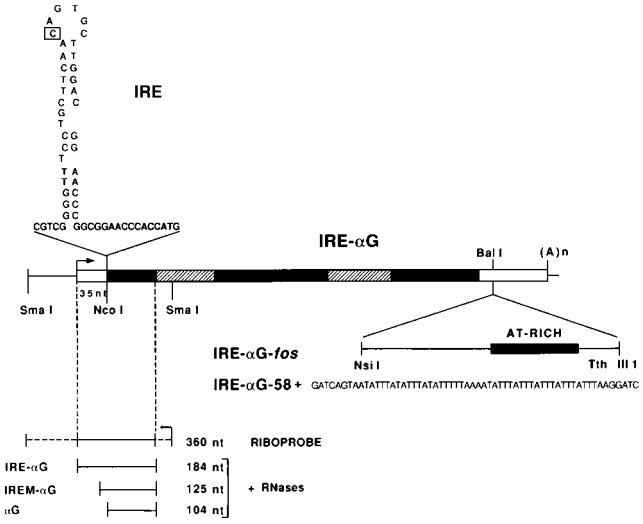

FIG. 1. Structures of the IRE–α-globin–3′ AU-rich recombinants. The c-*fos* and GM-CSF 3′ AT-rich elements were first cloned into the *Bal*I site of α-globin to generate pαG-*fos* and pαG-58+ (47). The 56-bp human ferritin IRE oligomer was next subcloned into the 5′ noncoding regions of pαG-*fos* and pαG-58+ to produce plasmids pIRE-αG-*fos* and pIRE-αG-58+, respectively. Plasmids pIREM-αG-*fos* and pIREM-αG-58+ were constructed in the same fashion, except that the first 5′ cytosine located in the IRE upper loop (boxed C) was deleted. The right-oriented arrow depicts the transcription initiation site. The filled and open boxes represent the exons, and the hatched boxes represent the introns. The noncoding regions are represented as open boxes. The riboprobe used to quantitate mRNA levels was designed by subcloning a *Sma*I-to-*Sma*I fragment obtained from pIRE-αG-*fos* (an α-globin–*fos* construct containing the IRE) into a pGEM-3 vector. T7 RNA polymerase produced a 360-nt RNA fragment complementary to the first exons of both pIRE-αG-*fos* and pIRE-αG-58+ transcripts. Following RNase mapping, pIRE-αG-*fos* and pIRE-αG-58+ mRNAs protected a 184-nt fragment, pIREM-αG-*fos* mRNA protected a 125-nt fragment, and pαG-58+ mRNA protected a 104-nt fragment.

other hydrophilic chelators, can enter the cell and chelate the intracellular pool of iron (13). Twenty-four hours after transfection, the cells were washed and 100 μM desferrioxamine was added to the cellular milieu. Because more than 16 h is required for the drug to attain its maximal effect, the cells were incubated in the presence of the iron chelator for at least 18 h (13). At the end of this treatment, the decay rates of transcribed mRNAs were analyzed by adding 10 μg of the transcriptional blocker actinomycin D per ml for increasing time periods ranging from 0 to 120 min. Total cytoplasmic RNA was harvested, and quantitative RNase mapping was performed with the 5′ pSIRE riboprobe. A β-globin riboprobe was also generated to measure β-globin mRNA levels.

Unexpectedly, desferrioxamine treatment fully prevented rapid mRNA degradation targeted by either ARE subset (Fig. 2). After 18 h of preincubation with the iron chelator, both pIRE-αG-*fos* and pIRE-αG-58+ mRNAs attained elevated steady-state levels and remained highly stable following inhibition of translation and arrest of transcription. The single 184-nt protected fragment corresponding to either RNA population conserved the same intensity throughout the experiment (Fig. 2A, lanes 1 to 6 [both panels]). Densitometric scanning revealed that pIRE-αG-*fos* and pIRE-αG-58+ mRNA levels were more than 90% of the original levels after a 2-h actinomycin D chase (Fig. 2C). Quantitation of β-globin messenger levels showed that transfection efficiencies and RNA recoveries were comparable in all mRNA samples tested (Fig. 2B). When a 4-h actinomycin D chase was performed, pIRE-αG-*fos* and pIRE-αG-58+ mRNA levels measured more than

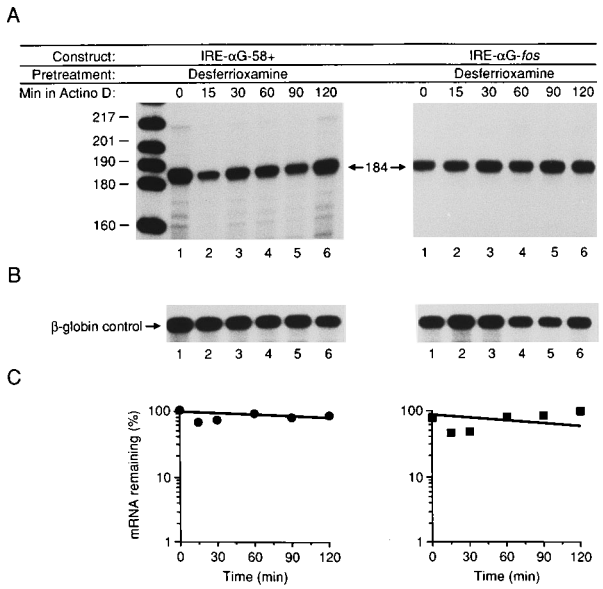

FIG. 2. Iron deprivation prevents rapid pIRE-αG-*fos* mRNA and pIRE-αG-58+ mRNA degradation. Sixteen hours after transfection of plasmids pIRE-αG-58+ and pIRE-αG-*fos* in NIH 3T3 cells, the cells were washed and incubated for 18 h in medium containing 100 μM desferrioxamine. (A) Quantitative mRNA analysis. Total cytoplasmic RNA was isolated at the indicated times after the addition of actinomycin D (10 μg/ml). RNA samples (10 μg) were analyzed with the 5′ riboprobe. RNase protection assays revealed a 184-nt protected fragment. Arrows indicate protected pIRE-αG-58+ and pIRE-αG-*fos* mRNA fragments. Sizes of fragments (in nucleotides) are indicated on the left. (B) RNase protection analysis of control β-globin mRNA. Plasmid pHβ1 was cotransfected with chimeric α-globin DNA constructs, and RNA (10 μg) was probed as described in Materials and Methods. (C) Decay rates of pIRE-αG-58+ (left) and pIRE-αG-*fos* (right) mRNAs. The intensity of the 184-nt protected fragment was measured by densitometric scanning, standardized by using the β-globin mRNA signal, and plotted. Each time point represents the mean of values measured in three separate experiments using different DNA preparations. The half-lives of pIRE-αG-58+ and pIRE-αG-*fos* transcripts were both estimated to be more than 120 min.

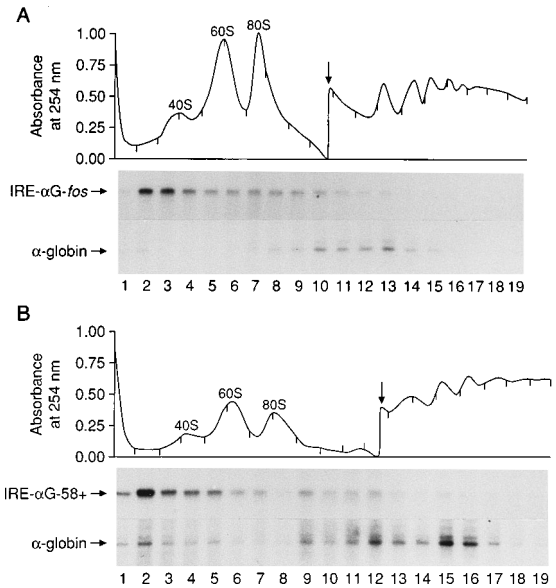

FIG. 3. Iron deprivation sequesters pIRE-αG-58+ and pIRE-αG-*fos* mRNAs from polysomes. Polysomal distribution of pIRE-αG-58+, pIRE-αG-*fos*, and α-globin transcripts in desferrioxamine-treated cells. Subconfluent NIH 3T3 cells were transiently transfected with pαG and with either pIRE-αG-*fos* (A) or pIRE-αG-58+ (B). Sixteen hours after transfection, the cells were washed and incubated for 18 h in DMEM containing the iron chelator, desferrioxamine, at a concentration of 100 μM. Cytoplasmic lysates were fractionated by sedimentation on a 15 to 40% sucrose gradient. Elution profiles were determined by continuous UV absorbance (254 nm) spectroscopy during fraction collection. The tops of the gradients are on the left. Absorbance peaks corresponding to 40S, 60S, and 80S ribosomal particles are indicated. Vertical arrows on elution graphics indicate that sensitivity of the absorbance monitor was increased by twofold (lanes 10 [A] or 12 [B] to 19). RNA was isolated from each fraction and hybridized with the 5′ pSIRE riboprobe described in the legend to Fig. 1. As expected, RNase digestion, electrophoresis, and autoradiography revealed a 184-nt protected fragment corresponding to pIRE-αG-*fos* (A) or pIRE-αG-58+ (B) mRNA and a 104-nt protected band corresponding to α-globin mRNA.

80% of their steady-state values (data not shown). Repetition of these experiments confirmed that desferrioxamine treatment always fully impeded rapid mRNA degradation.

To ascertain that the arrest of degradation resulted from complete sequestration of these mRNAs in the RNP pool, we next analyzed the polysomal distribution of pIRE-αG-*fos* and pIRE-αG-58+ transcripts in desferrioxamine-treated cells (Fig. 3). pIRE-αG-*fos* or pIRE-αG-58+ DNAs were transfected in NIH 3T3 cells along with the internal α-globin control, pαG. Twenty-four hours after transfection, 100 μM desferrioxamine was added to the cellular milieu and the incubation was pursued for 18 h. Cells were lysed, and cytoplasmic extracts were sedimented by centrifugation through a 15 to 40% (wt/vol) linear sucrose gradient. Polysomal profiles were established by monitoring protein A_{254} while the gradients were undergoing fractionation. Following RNA isolation, total amounts of pIRE-αG-*fos*, pIRE-αG-58+, and pαG transcripts were measured simultaneously in each fraction by RNase mapping, using the pSIRE riboprobe. The two IRE-derived and pαG mRNAs were detected as 184- and 104-nt protected fragments, respectively (Fig. 3).

As shown in Fig. 3, our results demonstrate that iron starvation induced by desferrioxamine treatment sequestered both pIRE-αG-*fos* (Fig. 3A) and pIRE-αG-58+ (Fig. 3B) transcripts in low-density RNP fractions away from denser polyribosomes. For example, more than 95% of the total amounts of pIRE-αG-*fos* and pIRE-αG-58+ mRNAs was detected in fractions 2 to 9 (Fig. 3, lanes 2 to 9), which corresponds to 40S, 60S, and 80S particles. Such sedimentation profiles are expected for mRNA populations that are not actively translated. On the other hand, α-globin mRNA sedimented faster than chimeric IRE messengers and was associated essentially with high-density polysomes (Fig. 3, lanes 9 to 16). This sedimentation pattern is as anticipated for this efficiently translated mRNA with several ribosomes attached to its 429-nt coding frame.

These results suggest that rapid messenger degradation mediated by either ARE subset is a translation-dependent mechanism that may be blocked by sequestration of recombinant mRNAs away from polyribosomes. An alternative explanation for such data is that the activity of soluble ribonucleases may be repressed by low iron availability.

Destabilizing activity of 3′ AREs is independent of iron availability. To investigate the presence of iron-dependent nucleases, we next tested the effect of desferrioxamine treatment on the turnover rate of messengers transcribed from the parental plasmid pαG-58+. Because these transcripts do not harbor a 5′ IRE, their translation efficiency is not affected by altering intracellular iron levels. In desferrioxamine-treated cells, pαG-58+ mRNA instability should not be affected unless RNase activity is downregulated by low intracellular iron levels.

Plasmid pαG-58+ was transiently transfected into NIH 3T3 cells along with pHβ1 as the control DNA. Twenty-four hours later, the cells were washed and 100 μM desferrioxamine was

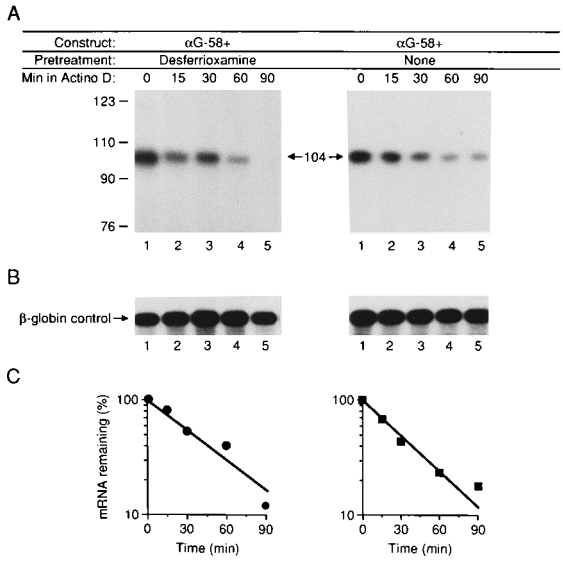

FIG. 4. The stabilizing effect of desferrioxamine is specific to transcripts harboring an IRE in their 5′ UTR. Plasmid pαG-58+ was transiently transfected in NIH 3T3 cells. Sixteen hours later, the cells were washed and incubated for 18 h in DMEM with or without desferrioxamine (100 μM). Actinomycin D (10 μg/ml) was then added to the cellular milieu, and the cells were incubated in the presence of the transcriptional inhibitor for increasing times ranging from 15 to 90 min before RNA harvesting. (A) RNase protection analysis of pαG-58+ transcripts. Ten micrograms of total cytoplasmic RNA was hybridized with the 5′ specific riboprobe. Digestion of samples by RNases A and T_1 protected a 104-nt fragment. Sizes of fragments (in nucleotides) are indicated on the left. (B) Signals of the control β-globin mRNA originating from cotransfection of pHβ1 with pαG-58+. (C) Decay rates of pαG-58+ mRNA in cells treated in the presence (left) or absence (right) of the iron chelator desferrioxamine. Measurement and calculation were done as described in the legend to Fig. 2. In both cases, mRNA half-lives were estimated to be less than 40 min. The transcript pαG-58+ is an α-globin mRNA that contains the GM-CSF destabilizing ARE in its 3′ UTR but does not harbor a 5′ IRE.

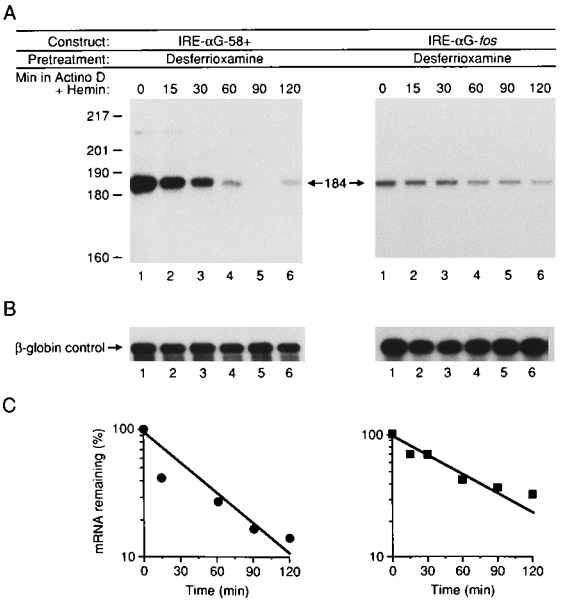

FIG. 5. Addition of iron to desferrioxamine-treated cells restores rapid degradation of pIRE-αG-*fos* and pIRE-αG-58+ mRNAs. Plasmid pIRE-αG-*fos* or pIRE-αG-58+ was transiently transfected in NIH 3T3 cells. Sixteen hours after transfection, 100 μM desferrioxamine was added and incubation was pursued for 18 h. The cells were then washed and treated simultaneously with the transcription inhibitor actinomycin D (10 μg/ml) and with hemin (100 μM) as a source of iron for increasing times of 15 to 120 min before RNA isolation. (A) Analysis of pIRE-αG-*fos* and pIRE-αG-58+ mRNA levels. Equal amounts (10 μg) of total cytoplasmic RNA were analyzed by RNase protection and gel electrophoresis. RNase protection assays revealed a 184-nt protected fragment. Sizes of fragments (in nucleotides) are indicated on the left. (B) Quantitation of control β-globin mRNA. (C) Decay analysis of pIRE-αG-58+ (left) and pIRE-αG-*fos* (right) mRNAs. Band intensities were quantitated by densitometric scanning and normalized to those for β-globin mRNA, as described in the legend to Fig. 2.

added for an 18-h incubation. The stability of the derived mRNAs was then measured by performing a 90-min actinomycin D chase followed by quantitative assessment of cytoplasmic mRNA levels. As depicted in Fig. 4A, low intracellular iron levels did not alter the high lability of the pαG-58+ mRNA. In cells pretreated with desferrioxamine, pαG-58+ mRNA was rapidly degraded following the addition of actinomycin D. Only a faint protected fragment was detected after a 60-min incubation with actinomycin D (Fig. 4A, left panel, lane 4). This band corresponded to less than 40% of original pαG-58+ mRNA levels measured before the addition of the transcriptional blocker (Fig. 4C). After a 90-min incubation with actinomycin D, pαG-58+ mRNA was completely degraded (Fig. 4A, left panel, lane 5). Under conditions of low iron availability, the pαG-58+ mRNA decay rate thus exhibited a degradation profile identical to its pattern under conditions of physiological iron concentrations with similar half-lives, estimated at less than 40 min in either condition (Fig. 4C). β-Globin control mRNAs demonstrated that comparable mRNA amounts were tested in the different samples (Fig. 4B). Under conditions of low intracellular iron availability, pαG-*fos* parental mRNA with no 5′ IRE also displayed high lability (data not shown).

From these results, we conclude that *trans*-acting factors involved in rapid mRNA degradation mediated by 3′ AREs are insensitive to iron manipulation. Consequently, desferrioxamine-induced stabilization of pIRE-αG-58+ and pIRE-αG-*fos* mRNAs, as shown in Fig. 2, ensues from messenger sequestration away from polyribosomes.

Redistribution of messengers to polysomes restores rapid mRNA degradation mediated by 3′ AREs. Our results demonstrate that mRNAs containing iterated AUUUA motifs within UUAUUUAUU nonamers failed to be rapidly degraded when not associated with polysomes. To provide further evidence for this translation-dependent decay mechanism, we reasoned that in cells pretreated with desferrioxamine, an iron supply should induce the redistribution of the chimeric transcripts to polyribosomes and concomitantly restore their instability.

Plasmid pIRE-αG-*fos* or pIRE-αG-58+ was transfected into NIH 3T3 cells along with pHβ1. Sixteen hours after transfection, the cells were incubated with 100 μM desferrioxamine for 18 h. To test for reinitiation of translation, the cells were washed free of desferrioxamine and treated simultaneously with 100 μM hemin, as a source of iron, and 10 μg of actinomycin D per ml for increasing time periods ranging from 0 to 120 min. RNA was harvested and quantitated by RNase protection. As shown in Fig. 5, the addition of hemin to cells pretreated with desferrioxamine restored a high level of instability to both pIRE-αG-*fos* and pIRE-αG-58+ mRNAs. These transcripts decayed rapidly following the arrest of transcription and reinitiation of translation. Two hours after the combined addition of hemin and actinomycin D, steady-state levels of pIRE-αG-*fos* and pIRE-αG-58+ transcripts had been degraded by almost 70 and 85%, respectively (Fig. 5A, lanes 6 [both panels]). As measured by densitometric scanning, pIRE-αG-58+ and pIRE-αG-*fos* mRNAs displayed half-lives of less than 30 and 45 min, respectively (Fig. 5C). In iron-supplemented cells, the half-lives of these two mRNA populations

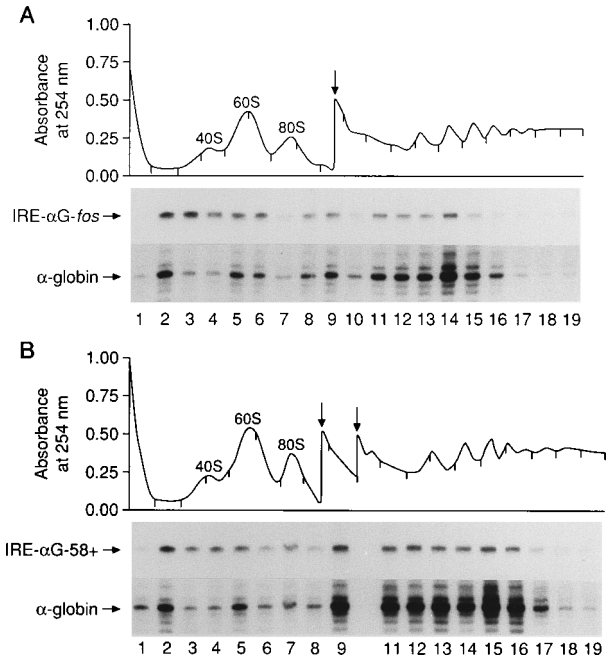

FIG. 6. The addition of hemin to iron-depleted cells induced redistribution of pIRE-αG-*fos* and pIRE-αG-58+ mRNAs to polysomes. Polysomal distribution of pIRE-αG-*fos*, pIRE-αG-58+, and α-globin transcripts in iron-repleted cells. NIH 3T3 cells were transiently transfected with pαG and either pIRE-αG-*fos* (A) or pIRE-αG-58+ (B). Sixteen hours later, 100 μM desferrioxamine was added and incubation was pursued for 18 h. The cells were then washed and treated with hemin (100 μM) for 2 h before lysis. Polysomal distribution analysis was done as described in the legend to Fig. 3. Vertical arrows indicate that sensitivity of the absorbance monitor was increased by twofold (lanes 9 to 17).

were thus highly similar to those of pαG-58+ (Fig. 4) and pαG-*fos* transcripts (47, 50), both observed at approximately 30 min, or to other chimeric mRNAs harboring 3′ AREs (58). Quantitation of control β-globin mRNA revealed that hemin treatment did not alter transfection efficiencies or mRNA recoveries (Fig. 5B).

To confirm that the addition of hemin to iron-starved cells induced redistribution of pIRE-αG-*fos* and pIRE-αG-58+ mRNAs to polysomes, we next analyzed the cytoplasmic location of these transcripts in cells treated successively with desferrioxamine followed by hemin. NIH 3T3 cells were transfected with pIRE-αG-*fos* or pIRE-αG-58+ along with pαG DNAs. Iron depletion was achieved by incubating the cells for 18 h in the presence of 100 μM desferrioxamine. At the end of this incubation, the iron chelator was removed from the culture medium and 100 μM hemin was added for a 2-h period before cell lysis. Cytoplasmic supernatants were sedimented through sucrose gradients and fractionated as previously described. Polysomal profiles were obtained by continuous A_{254} monitoring followed by RNA isolation and quantitation, using the pSIRE probe. As depicted in Fig. 6, pIRE-αG-*fos* and pIRE-αG-58+ transcripts were evenly distributed along the gradients. Comparable amounts of pIRE-αG-*fos* mRNA (Fig. 6A) or pIRE-αG-58+ mRNA (Fig. 6B) from fractions 2 to 16 were observed. Control α-globin mRNAs were also present in all fractions tested and exhibited distribution patterns highly similar to those of pIRE-αG-*fos* and pIRE-αG-58+ transcripts (Fig. 6). This polysomal distribution is characteristic of transcripts being actively translated; it corresponds to mRNAs associated with 40S and 60S particles as well as to monoribosomes and polyribosomes. Such profiles are also reminiscent of experiments showing that ferritin protein biosynthesis is reactivated following redistribution of its mRNA from nonpolysome to polysome pools upon hemin induction (5, 48). pαG-*fos* or pαG-58+ transcripts also displayed analogous mRNA distributions when tested under similar conditions (results not shown). As both pIRE-αG-*fos* and pIRE-αG-58+ mRNA populations exhibited polysomal profiles highly similar to those of control α-globin transcripts, we conclude that the addition of hemin to cells preincubated in the presence of desferrioxamine induced the translocation of pIRE-αG-*fos* and pIRE-αG-58+ mRNAs to high-density polyribosomes and restored high mRNA lability conferred by either the c-*fos* or GM-CSF ARE.

A single-point deletion in the IRE abolishes targeted sequestration and concomitant mRNA stabilization. The IRE is a *cis*-acting RNA sequence defined as a moderately stable stem-loop structure consisting of 28 highly conserved nucleotides (6). Specific deletions in the loop reduce the affinity with which IRE-BP attaches to IRE, leading to an inability of IRE to regulate translation (6, 49). To verify that the IRE's effect was specific to its role as a *cis*-acting translational regulator, we studied the turnover rate of a mutant form of IRE–α-globin–ARE transcripts in which the first 5′ cytosine residue (underlined) present at the top of the 6-nt IRE stem-loop structure (CAGUGC) had been deleted. This recombinant, originating from plasmid pαG-*fos*, was named pIREM-αG-*fos* (Fig. 1).

We first analyzed the stability of pIREM-αG-*fos* mRNA in iron-depleted cells. NIH 3T3 fibroblasts were transiently transfected with pIREM-αG-*fos* and treated with desferrioxamine for 18 h. Actinomycin D was added, and the incubation was pursued for increasing times ranging from 0 to 120 min. Transcripts were then quantitated by RNase protection. As depicted in Fig. 7, iron chelation did not alter the instability of pIREM-αG-*fos* mRNAs. The transcripts were rapidly degraded, and less than 20% of their original levels remained after a 2-h incubation in desferrioxamine-treated cells (Fig. 7A). The pIREM-αG-*fos* mRNA half-life, estimated at less than 45 min (Fig. 7C), was thus highly similar to that of pαG-58+ mRNA measured under conditions of low iron availability (Fig. 4).

To ascertain that the single cytosine deletion in the IRE stem-loop structure was sufficient to prevent mRNA sequestration, we then determined the cytoplasmic location of pIREM-αG-*fos* mRNA in desferrioxamine-treated cells. The inherent capacity of the 5′ pSIRE riboprobe to detect simultaneously pIRE and pIREM-derived mRNAs allowed us to transfect pIRE-αG-*fos* along with pIREM-αG-*fos* to compare the polysomal distribution of their respective mRNAs in the same experiment. Following transient transfection, NIH 3T3 cells were treated for 18 h with 100 μM desferrioxamine and lysed; then the extracts were sedimented through a 15 to 40% sucrose gradient as previously described. As expected, pIRE-αG-*fos* mRNA remained associated with low-density 40S and 60S particles (Fig. 8, lanes 1 to 6) corresponding to subribosomal proteins and RNP elements that included the IRE-BP. On the other hand, pIREM-αG-*fos* transcripts were found entirely in heavier fractions (Fig. 8, lanes 11 to 19) corresponding to high-density polysomes. Such data indicate that pIREM-αG-*fos* transcripts were transferred to active polyribosomes even when intracellular iron concentrations had been greatly reduced. Identical results were obtained when the IREM mutation was introduced into pαG-58+ mRNA (data not shown). These results indicate that a single point deletion in the 5′ IRE is sufficient to abolish IRE-targeted sequestration, which concomitantly stabilizes the mRNAs harboring 3′ AREs.

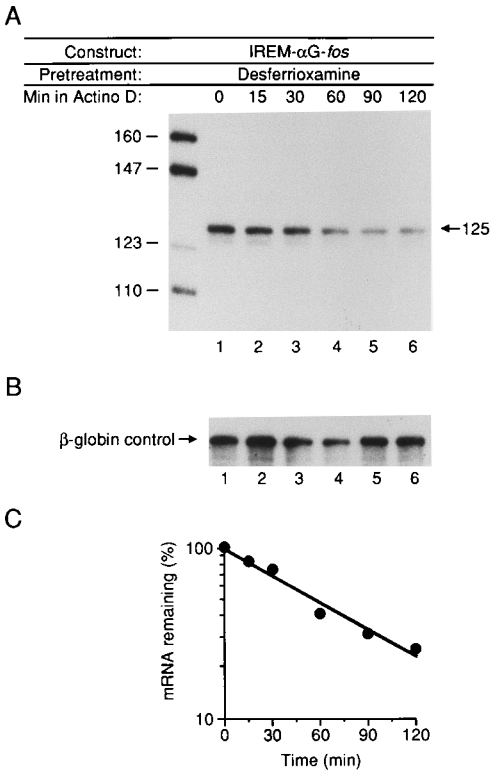

FIG. 7. A point deletion in the IRE restores rapid degradation of a mutant form of pIRE-αG-*fos* mRNA in desferrioxamine-treated cells. Plasmid pIREM-αG-*fos* containing a point deletion in the IRE, as described in the legend to Fig. 1, was transiently transfected in NIH 3T3 cells. Sixteen hours after transfection, the cells were washed and incubated for 18 h in DMEM containing 100 μM desferrioxamine. (A) Total cytoplasmic RNA was isolated at the indicated times after treatment with 10 μg of actinomycin D per ml. Equal amounts of RNA (10 μg) were hybridized to the 5′ pSIRE riboprobe and digested by RNases A and T_1. Electrophoresis and autoradiography revealed a 125-nt protected fragment (indicated by an arrow) corresponding to pIREM-αG-*fos* mRNA. Sizes of fragments (in nucleotides) are indicated on the left. (B) Control plasmid pHβ1 was cotransfected with pIREM-αG-*fos*, and mRNA was quantitated by RNase protection analysis. (C) Decay rate of pIREM-αG-*fos* mRNA in desferrioxamine-treated cells. The intensity of the pIREM-αG-*fos* bands was corrected for RNA content in each lane by comparison with the β-globin signal. The percentage of the signal was plotted logarithmically against time, as indicated in the legend to Fig. 2.

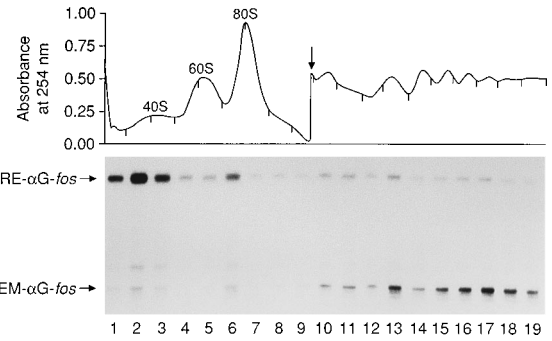

FIG. 8. A point deletion in the IRE abolishes iron-modulated sequestration of mutant pIRE-αG-*fos* transcripts. Polysomal distribution of pIREM-αG-*fos* and pIRE-αG-*fos* mRNAs in desferrioxamine-treated cells. Subconfluent NIH 3T3 cells were simultaneously transfected with pIREM-αG-*fos* and pIRE-αG-*fos*. Sixteen hours later, the cells were washed and incubated for 18 h in DMEM containing 100 μM desferrioxamine. Polysome profiles of cytoplasmic lysates were generated by sedimentation through a 15 to 40% sucrose gradient followed by continuous UV absorbance (254 nm) spectroscopy during fraction collection. The top of the gradient is on the left. Positions of the 40S, 60S, and 80S ribosomal subunits are marked. The vertical arrow indicates that the sensitivity of the absorbance monitor was increased by twofold (lanes 10 to 19). RNA was extracted from each fraction, hybridized with the 5′ pSIRE riboprobe, and digested with RNases. Autoradiography revealed two protected fragments: the 184-nt fragment, which corresponded to pIRE-αG-*fos* mRNA, and the 125-nt fragment, which recognized pIREM-αG-*fos* mRNA.

DISCUSSION

It has been proposed that the different ARE subsets that mediate the degradation of many short-lived mRNAs function through distinct decay pathways. To investigate the specificity of these pathways, we exploited the properties of the ferritin IRE to design a unique mRNA shuttling system in which the translation of specific mRNA populations was controlled solely by changes in intracellular iron availability. In combination with polysomal profile analysis, this system allowed us to closely monitor the location of the transcripts. Here we demonstrated that (i) iron deprivation blocked the accessibility of IRE–α-globin–ARE mRNAs to ribosomes and concomitantly stabilized those transcripts, (ii) the addition of hemin to iron-depleted cells induced translocation of mRNA toward polyribosomes and restored their rapid degradation, (iii) the ARE destabilizing activity was independent of iron availability, and (iv) the c-*fos* and GM-CSF AREs behaved identically. Our data therefore support a model in which the two major 3′ ARE subsets mediate selective mRNA degradation, coupled to ongoing translation, through highly similar, if not identical, polyribosome-associated mechanisms.

Our finding that rapid mRNA decay directed by 3′ AREs requires translation is consistent with experiments showing that premature translational termination induces rapid mRNA turnover in *Saccharomyces cerevisiae* (34). The present data are also consistent with the recent findings of Aharon and Schneider (1), who observed that relief of translation inhibition by insertion of an internal ribosome entry site, downstream of a 5′ inhibitory sequence, restored high lability to transcripts harboring the GM-CSF ARE linked to the hepatitis B virus S-antigen coding region. The present experiments thus provide evidence that c-*fos* and GM-CSF AREs conferred high mRNA instability only upon redistribution of the transcripts to high-density polyribosomes.

Using a highly similar system, Koeller et al. previously proposed that the destabilization triggered by the c-*fos* ARE is not linked to translation of the transcript but, rather, requires *trans*-acting labile proteins (30). After stably transfecting mouse B6 fibroblasts with a chimeric DNA encoding the transferrin receptor coding sequence harboring the ferritin IRE in its 5′ UTR and the c-*fos* ARE in its 3′ UTR, these authors found that this highly unstable mRNA is, as expected, stabilized by cycloheximide. In contrast to our data, however, Koeller et al. demonstrated that desferrioxamine treatment did not alter the rapid turnover rate of this recombinant transcript, although it stopped protein synthesis originating from the mRNA. Such a discrepancy may be explained by as yet unrecognized *cis*-acting determinants present in the α-globin and/or transferrin receptor mRNA sequences or by dissimilarities between the different cell lines used to measure mRNA turnovers. These *cis*-acting sequences may be similar, for example, to the destabilizing elements found in the c-*fos* and c-*myc* mRNA coding regions (60, 66) or to ARE-adjacent instability determinants in the GM-CSF and urokinase-type plasminogen activator 3′ UTR which have been recently characterized (25, 44). Extensive studies of globin messengers, however, excluded such instability determinants in the coding region of the

mRNA (28, 63) and further revealed an erythroid cell-specific stability element present in the 3′ UTR of α_2-globin mRNA (64). The second possibility is expression of an alternative translation-independent degradative pathway in stably transfected mouse B6 fibroblasts. Further experimentation using identical recombinants with different transfection methods in various cell lines may elucidate these differences.

Although the present study clearly supports a translation-dependent mechanism of degradation, our results do not exclude the participation of labile cycloheximide-sensitive factors associated with polyribosomes. One recent study suggested that GM-CSF ARE-mediated mRNA instability in the baby hamster kidney cell line tsAF8 requires the translation-dependent assembly of a >20S degradation complex (56). If present in NIH 3T3 cells, this putative >20S complex would have been detected by a shift, or a broadening, of at least two fractions of the IRE transcripts toward denser regions of the gradients. However, comparison of the sedimentation profiles of pIRE-αG-*fos* or pIRE-αG-58+ mRNAs and α-globin control transcripts upon their redistribution to polyribosomes revealed that these profiles could be superimposed. Monitoring the distribution patterns of parental pαG-58+ mRNAs and α-globin transcripts also unveiled identical profiles (31a). The >20S complex may thus represent a cell-specific factor and/or may be coupled to polysomes for only a very transient period that is too brief to be detected using the IRE shuttling system in NIH 3T3 cells. This second possibility is favored by observations that chimeric β-globin RNAs harboring the GM-CSF ARE displayed half-lives of more than 150 min in tsAF8 cells (56), whereas half-lives of similar fusion mRNAs were estimated at less than 30 min in exponentially growing NIH 3T3 cells (1, 47, 50, 58). Exploiting the IRE shuttling system should help to unmask the roles of many specific ARE-binding complexes, which remain elusive.

Although much progress has been made in characterizing the *cis*- and *trans*-acting elements involved in the regulation of mRNA decay, we are still far from a detailed description of the pathways that would fully explain how lymphokines and early-response mRNAs are selectively targeted for rapid degradation. Our results clearly demonstrate, however, that translation is essential to ARE-mediated destabilization. In this context, two mechanisms can be envisaged to explain such a requirement. The first would imply a mechanical participation of translationally active polysomes that would permit the unwinding of mRNA secondary structures or the displacement of some mRNA binding factors, allowing a subsequent ribonucleolytic attack by AU-rich specific or nonspecific *trans*-acting factors. The second model is one in which a component of the translational apparatus itself is essential to mRNA degradation mediated by 3′ AREs. The RNase activity of such a component could therefore be activated or inhibited by the presence of AU-rich binding factors (7, 8, 10, 18, 37, 38, 67, 68). Experiments performed with *S. cerevisiae* showing that the shortening of poly(A) tails requires the poly(A)-binding protein (53) and indicating a role for 3′ UTR in translational initiation (26, 42, 51) support this model. As one of the first steps involved in ARE-mediated mRNA decay is the accelerated deadenylation of the transcripts prior to degradation of the transcribed portion of the message (11, 59, 65), a *trans*-acting factor(s) similar to yeast poly(A) ribonuclease involved in poly(A)-binding protein-dependent shortening of poly(A) tails and translation initiation (54) and/or an associated factor(s) may be expected to be found in higher eukaryotes. Further determination of the site of poly(A) shortening will thus have a major impact on our understanding of the commitment of an mRNA to degradation, and future work must establish whether the ARE-mediated deadenylation process is itself a polysome-associated process. The IRE shuttling system offers a powerful approach for investigating the mechanism by which the early poly(A) tail loss occurs and for studying the many other aspects of mRNA degradation.

ACKNOWLEDGMENTS

We are grateful to Geneviève Laflamme for technical assistance, particularly during the polysomal distribution experiments.

This work was supported by a grant from the Medical Research Council of Canada (MRC) and was initiated in the Laboratoire de Neurogénétique Moléculaire du Centre de Recherche Université Laval-Robert Giffard. Eric Winstall was supported by a studentship provided by Fonds pour la Formation de Chercheurs et l'Aide à la Recherche (FCAR). Vincent Raymond is an MRC scholar.

REFERENCES

1. **Aharon, T., and R. J. Schneider.** 1993. Selective destabilization of short-lived mRNAs with the granulocyte-macrophage colony-stimulating factor AU-rich 3′ noncoding region is mediated by a cotranslational mechanism. Mol. Cell. Biol. **13:**1971–1980.
2. **Altus, M. S., and Y. Nagamine.** 1991. Protein synthesis inhibition stabilizes urokinase-type plasminogen activator mRNA. J. Biol. Chem. **266:**21190–21196.
3. **Atwater, J. A., R. Wisdom, and I. M. Verma.** 1990. Regulated mRNA stability. Annu. Rev. Genet. **24:**519–541.
4. **Ausubel, F. M., R. Brent, R. E. Kingston, D. D. Moore, J. G. Seidman, J. A. Smith, and K. Struhl (ed.).** 1987. Current protocols in molecular biology, vol. I. Greene Publishing Associates and Wiley-Interscience, New York.
5. **Aziz, N., and H. N. Munro.** 1986. Both subunits of rat liver ferritin are regulated at a translational level by iron induction. Nucleic Acids Res. **14:**915–927.
6. **Bettany, A. J. E., R. S. Eisenstein, and H. N. Munro.** 1992. Mutagenesis of the iron-regulatory element further defines a role for RNA secondary structure in the regulation of ferritin and transferrin receptor expression. J. Biol. Chem. **267:**16531–16537.
7. **Bohjanen, P. R., B. Petryniak, C. H. June, C. B. Thompson, and T. Lindsten.** 1991. An inducible cytoplasmic factor (AU-B) binds selectively to AUUUA multimers in the 3′ untranslated region of lymphokine mRNA. Mol. Cell. Biol. **11:**3288–3295.
8. **Bohjanen, P. R., B. Petryniak, C. H. June, C. B. Thompson, and T. Lindsten.** 1992. AU RNA-binding factors differ in their binding specificities and affinities. J. Biol. Chem. **267:**6302–6309.
9. **Borelli, E., R. Hen, and P. Chambon.** 1984. The adenovirus-2 E1A products repress stimulation of transcription by enhancers. Nature (London) **312:**608–612.
10. **Brewer, G.** 1991. An A+U-rich element RNA-binding factor regulates c-*myc* mRNA stability in vitro. Mol. Cell. Biol. **11:**2460–2466.
11. **Brewer, G., and J. Ross.** 1988. Poly(A) shortening and degradation of the 3′ A+U-rich sequences of human c-*myc* mRNA in a cell-free system. Mol. Cell. Biol. **8:**1697–1708.
12. **Brewer, G., and J. Ross.** 1989. Regulation of c-*myc* mRNA stability in vitro by a labile destabilizer with an essential nucleic acid component. Mol. Cell. Biol. **9:**1996–2006.
13. **Bridges, K. R., and A. Cudkowicz.** 1984. Effect of iron chelators on the transferrin receptor in K562 cells. J. Biol. Chem. **259:**12970–12977.
14. **Caput, D., B. Beutler, K. Hartog, R. Thayer, S. Brown-Shimer, and A. Cerami.** 1986. Identification of a common nucleotide sequence in the 3′-untranslated region of mRNA molecules specifying inflammatory mediators. Proc. Natl. Acad. Sci. USA **83:**1670–1674.
15. **Casey, J. L., M. W. Hentze, D. M. Koeller, S. W. Caughman, T. A. Rouault, R. D. Klausner, and J. B. Harford.** 1988. Iron-responsive elements: regulatory RNA sequences that control mRNA levels and translation. Science **240:**924–928.
16. **Favaloro, J., R. H. Treisman, and R. Kamen.** 1981. Transcription maps of polyoma virus-specific RNA: analysis by two-dimensional nuclease S1 gel mapping. Methods Enzymol. **65:**718–749.
17. **Foulkes, N. S., F. Schlotter, P. Pévet, and P. Sassone-Corsi.** 1993. Pituitary hormone FSH directs the CREM functional switch during spermatogenesis. Nature (London) **362:**264–267.
18. **Gillis, P., and J. S. Malter.** 1991. The adenosine-uridine binding factor recognizes the AU-rich elements of cytokine, lymphokine, and oncogene mRNAs. J. Biol. Chem. **266:**3172–3177.
19. **Goossen, B., and M. W. Hentze.** 1992. Position is the critical determinant for function of iron-responsive elements as translational regulators. Mol. Cell. Biol. **12:**1959–1966.
20. **Graham, R., and A. J. Van-Der-Eb.** 1973. A new technique for the assay of infectivity of human adenovirus 5 DNA. Virology **52:**456–467.

21. **Greenberg, M. E., and J. G. Belasco.** 1993. Control of the decay of labile protooncogene and cytokine mRNAs, p. 199–219. *In* J. Belasco and G. Brawerman (ed.), Control of messenger RNA stability, vol. 1. Academic Press, San Diego, Calif.
22. **Hentze, M. W.** 1991. Determinants and regulation of cytoplasmic mRNA stability in eukaryotic cells. Biochim. Biophys. Acta **1090:**281–292.
23. **Hentze, M. W., S. W. W. Caughman, T. A. Rouault, J. G. Barriocanal, A. Dancis, J. H. Harford, and R. D. Klausner.** 1987. Identification of the iron-responsive element for the translational regulation of human ferritin mRNA. Science **238:**1570–1573.
24. **Hentze, M. W., T. A. Rouault, S. W. Caughman, A. Dancis, J. B. Harford, and R. D. Klausner.** 1987. A cis-acting element is necessary and sufficient for translational regulation of human ferritin expression in response to iron. Proc. Natl. Acad. Sci. USA **84:**6730–6734.
25. **Iwai, Y., M. Bickel, D. H. Pluznik, and R. B. Cohen.** 1991. Identification of sequences within the murine granulocyte-macrophage colony-stimulating factor mRNA 3′-untranslated region that mediate mRNA stabilization induced by mitogen treatment of EL-4 thymoma cells. J. Biol. Chem. **266:** 17959–17965.
26. **Jackson, R. J., and N. Standart.** 1990. Do the poly(A) tail and 3′ untranslated region control mRNA translation? Cell **62:**15–24.
27. **Jones, T. R., and M. D. Cole.** 1987. Rapid cytoplasmic turnover of c-*myc* mRNA: requirement of the 3′ untranslated sequences. Mol. Cell. Biol. **7:**4513–4521.
28. **Kabnick, K. S., and D. E. Housman.** 1988. Determinants that contribute to cytoplasmic stability of human c-*fos* and α-globin mRNAs are located at several sites in each mRNA. Mol. Cell. Biol. **8:**3244–3250.
29. **Klausner, R. D., T. A. Rouault, and J. B. Harford.** 1993. Regulating the fate of mRNA: the control of cellular iron metabolism. Cell **72:**19–28.
30. **Koeller, D. M., J. A. Horowitz, J. L. Casey, R. D. Klausner, and J. B. Harford.** 1991. Translation and the stability of mRNAs encoding the transferrin receptor and c-*fos*. Proc. Natl. Acad. Sci. USA **88:**7778–7782.
31. **Kozak, M.** 1991. Structural features in eukaryotic mRNAs that modulate the initiation of translation. J. Biol. Chem. **266:**19867–19870.

31a. **Laflamme, G., and V. Raymond.** Unpublished data.

32. **Lagnado, C. A., C. Y. Brown, and G. J. Goodall.** 1994. AUUUA is not sufficient to promote poly(A) shortening and degradation of an mRNA: the functional sequence within AU-rich elements may be UUAUUUA(U/A)(U/A). Mol. Cell. Biol. **14:**7984–7995.
33. **Lee, W. M. F., C. Lin, and T. Curran.** 1988. Activation of the transforming potential of the human *fos* proto-oncogene requires message stabilization and results in increased amounts of partially modified *fos* protein. Mol. Cell. Biol. **8:**5521–5527.
34. **Leeds, P., S. W. Peltz, A. Jacobson, and M. R. Culbertson.** 1991. The product of the yeast UPF1 gene is required for rapid turnover of mRNAs containing a premature translational termination codon. Genes Dev. **5:**2303–2314.
35. **Lindsten, T., C. H. June, J. A. Ledbetter, G. Stella, and C. B. Thompson.** 1989. Regulation of lymphokine messenger RNA stability by a surface-mediated T cell activation pathway. Science **244:**339–343.
36. **Linial, M., N. Gunderson, and M. Groudine.** 1985. Enhanced transcription of c-*myc* in bursal lymphoma cells required continued protein synthesis. Science **230:**1126–1132.
37. **Malter, J. S.** 1989. Identification of an AUUUA-specific messenger RNA binding protein. Science **246:**664–666.
38. **Malter, J. S., and Y. Hong.** 1991. A redox switch and phosphorylation are involved in the post-translational up-regulation of the adenosine-uridine binding factor by phorbol ester and ionophore. J. Biol. Chem. **266:**3167–3171.
39. **Mellon, P., V. Parker, Y. Gluzman, and T. Maniatis.** 1981. Identification of DNA sequences required for transcription of the human α1-globin gene in a new SV40 host-vector system. Cell **27:**279–288.
40. **Mitchell, R. L., L. Zokas, R. D. Schreiber, and I. M. Verma.** 1985. Rapid induction of the expression of proto-oncogene *fos* during human monocytic differentiation. Cell **40:**209–217.
41. **Müllner, E. W., and L. C. Kühn.** 1988. A stem-loop in the 3′ untranslated region mediates iron-dependent regulation of transferrin receptor mRNA stability in the cytoplasm. Cell **53:**815–825.
42. **Munroe, D., and A. Jacobson.** 1990. mRNA poly(A) tail, a 3′ enhancer of translation initiation. Mol. Cell. Biol. **10:**3441–3455.
43. **Nair, A. P. K., S. Hahn, R. Banholzer, H. H. Hirsch, and C. Moroni.** 1994. Cyclosporin A inhibits growth of autocrine tumor cell lines by destabilizing interleukin-3 mRNA. Nature (London) **369:**239–242.
44. **Nanbu, R., P.-A. Menoud, and Y. Nagamine.** 1994. Multiple instability-regulating sites in the 3′ untranslated region of the urokinase-type plasminogen activator mRNA. Mol. Cell. Biol. **14:**4920–4928.
45. **Peppel, K., and C. Baglioni.** 1991. The AU-rich sequences in the 3′ untranslated region mediate the increased turnover of interferon mRNA induced by glucocorticoids. J. Exp. Med. **173:**349–355.
46. **Peppel, K., and C. Baglioni.** 1991. Deadenylation and turnover of interferon-β mRNA. J. Biol. Chem. **266:**6663–6666.
47. **Raymond, V., J. Atwater, and I. M. Verma.** 1989. Removal of an mRNA destabilizing element correlates with the increased oncogenicity of proto-oncogene *fos*. Oncogene Res. **5:**1–12.
48. **Rogers, J., and H. Munro.** 1987. Translation of ferritin light and heavy subunit mRNAs is regulated by intracellular chelatable iron levels in rat hepatoma cells. Proc. Natl. Acad. Sci. USA **84:**2277–2281.
49. **Rouault, T. A., M. W. Hentze, S. W. Caughman, J. B. Harford, and R. D. Klausner.** 1988. Binding of a cytosolic protein to the iron-responsive element of human ferritin messenger RNA. Science **241:**1207–1210.
50. **Roy, N., G. Laflamme, and V. Raymond.** 1992. 5′ untranslated sequences modulate rapid mRNA degradation mediated by 3′ AU-rich element in v-/c-*fos* recombinants. Nucleic Acids Res. **20:**5753–5762.
51. **Sachs, A.** 1990. The role of poly(A) in the translation and stability of mRNA. Curr. Opin. Cell Biol. **2:**1092–1098.
52. **Sachs, A. B.** 1993. Messenger RNA degradation in eukaryotes. Cell **74:**413–421.
53. **Sachs, A. B., and R. W. Davis.** 1989. Translation initiation and ribosomal biogenesis: involvement of a putative rRNA helicase and RPL46. Science **247:**1077–1079.
54. **Sachs, A. B., and J. A. Deardorff.** 1992. Translation initiation requires the PAB-dependent poly(A) ribonuclease in yeast. Cell **70:**961–973.
55. **Sambrook, J., E. F. Fritsch, and T. Maniatis.** 1989. Molecular cloning: a laboratory manual, 2nd ed., vol. II. Cold Spring Harbor Laboratory Press, Cold Spring Harbor, N.Y.
56. **Savant-Bhonsale, S., and D. W. Cleveland.** 1992. Evidence for instability of mRNAs containing AUUUA motifs mediated through translation-dependent assembly of a >20S degradation complex. Genes Dev. **6:**1927–1939.
57. **Schuler, G. D., and M. D. Cole.** 1988. GM-CSF and oncogene mRNA stabilities are independently regulated in *trans* in a mouse monocytic tumor. Cell **55:**1115–1122.
58. **Shaw, G., and R. Kamen.** 1986. A conserved AU sequence from the 3′-untranslated region of GM-CSF mRNA mediates selective mRNA degradation. Cell **46:**659–667.
59. **Shyu, A.-B., J. G. Belasco, and M. E. Greenberg.** 1991. Two distinct destabilizing elements in the c-*fos* message trigger deadenylation as a first step in rapid mRNA decay. Genes Dev. **5:**221–231.
60. **Shyu, A.-B., M. E. Greenberg, and J. G. Belasco.** 1989. The c-*fos* transcript is targeted for rapid decay by two distinct mRNA degradation pathways. Genes Dev. **3:**60–72.
61. **Stehle, J. H., N. S. Foulkes, C. A. Molina, V. Simonneaux, P. Pévet, and P. Sassone-Corsi.** 1993. Adrenergic signals direct rhythmic expression of transcriptional repressor CREM in the pineal gland. Nature (London) **365:**314–320.
62. **Van Beveren, C., F. Van Straaten, T. Curran, R. Müller, and I. M. Verma.** 1983. Analysis of FBJ-MuSV provirus and c-*fos* (mouse) gene reveals that viral and cellular *fos* gene products have different carboxy termini. Cell **32:**1241–1255.
63. **Volloch, V., and D. Housman.** 1981. Stability of globin mRNA in terminally differentiating murine erythroleukemia cells. Cell **23:**509–514.
64. **Weiss, I. M., and S. A. Liebhaber.** 1994. Erythroid cell-specific determinants of α-globin mRNA stability. Mol. Cell. Biol. **14:**8123–8132.
65. **Wilson, T., and R. Treisman.** 1988. Removal of poly(A) and consequent degradation of c-*fos* mRNA facilitated by 3′ AU-rich sequences. Nature (London) **336:**396–399.
66. **Wisdom, R., and W. Lee.** 1991. The protein-coding region of c-myc mRNA contains a sequence that specifies rapid mRNA turnover and induction by protein synthesis inhibitors. Genes Dev. **5:**232–243.
67. **You, Y., C.-Y. A. Chen, and A.-B. Shyu.** 1992. U-rich sequence-binding proteins (URBPs) interacting with a 20-nucleotide U-rich sequence in the 3′ untranslated region of c-*fos* mRNA may be involved in the first step of c-*fos* mRNA degradation. Mol. Cell. Biol. **12:**2931–2940.
68. **Zhang, W., B. J. Wagner, K. Ehrenman, A. W. Schaefer, C. T. DeMaria, D. Crater, K. DeHaven, L. Long, and G. Brewer.** 1993. Purification, characterization, and cDNA cloning of an AU-rich element RNA-binding protein, AUF1. Mol. Cell. Biol. **13:**7652–7665.
69. **Zubiaga, A. M., J. G. Belasco, and M. E. Greenberg.** 1995. The nonamer UUAUUUAUU is the key AU-rich sequence motif that mediates mRNA degradation. Mol. Cell. Biol. **15:**2219–2230.